Particle Accelerators, 1996, Vol. 54, pp. 167–181
Reprints available directly from the publisher
Photocopying permitted by license only

GEOMETRY OF ORBITS AND ACTION DIFFUSION FROM NORMAL FORMS IN NONLINEAR BEAM DYNAMICS

G. TURCHETTI

Dipartimento di Fisica and INFN, Via Irnerio 46, I-40126 Bologna, Italy

(Received 24 December 1995; in final form 24 December 1995)

The betatronic motion in a nonlinear magnetic lattice is described by the normal forms on the one turn map. The geometry of the orbits emerges from 3D sections or projections of the invariant manifolds. Methods to compute the invariant actions are presented and it is shown that the noise induced diffusion is described by a Fokker-Planck equation whose coefficients are analytically determined.

Keywords: Beam dynamics.

1 INTRODUCTION

Nonlinear effects in charged beams optical systems are introduced by the multipolar errors of the superconducting magnets.[1] The one turn map is known either by evaluating step by step the single elements transfer maps (tracking) or by a polynomial truncation. For hadron colliders with strong nonlinearities the normal forms have been proposed to recover a symplectic map with explicit symmetries from the truncated map.[2] The normal forms, first introduced in celestial mechanics for the long term analysis on comparable time scales, are complementary to tracking. The former is tailored to describe analytically the quasi-integrable dynamical structures, the latter to explore the strongly chaotic regions. The normal forms define a hamiltonian H, whose flow interpolates the orbits of the map just as the Fourier analysis on the tracking data; the interpolation by H is defined in the whole region where the normal forms hold, whereas the Fourier analysis has to be repeated for every orbit. The interpolation allows to compute the

tunes and the invariant actions, which are needed to investigate the resonance network. The interpolating hamiltonian H is also the starting point to treat the diffusion induced by stochastic perturbations of the lattice (ground motion, RF noise,..) or by a slow modulation (ripples of current in the quadrupoles). The evolution of the density distribution in action space is determined by a Fokker-Planck equation, whose coefficients are analytically determined by H.[3] The agreement found between the simulation and the Fokker-Planck solution for nonresonant 2D maps with noise and preliminary positive results on the resonant 2D maps suggest that the treatment of a 4D map describing a realistic lattice is possible.

2 ONE TURN MAP

We consider the transverse motion of particles near a reference closed orbit in a horizontal plane. In a frame (x, y, s), where s is the curvilinear abscissa and x, y are the horizontal and vertical coordinate, the orbit is defined by $x = x(s)$, $y = y(s)$ and $p_x = dx/ds$, $p_y = dy/ds$ are the corresponding momenta. The phase space vector $\mathbf{x}(s) = (x(s), p_x(s), y(s), p_y(s))$ at the entrance of a magnetic element of length ℓ is transformed into the vector $\mathbf{x}(s + \ell)$ at the exit of the same element by a symplectic transfer map M,

$$\mathbf{x}(s + \ell) = M(\mathbf{x}(s)) \tag{1}$$

since $\mathbf{x}(s)$ satisfies Hamilton's equations. If the lattice consists of m magnetic elements sitting in the arcs $[0, s_1], \ldots, [s_{m-1}, s_m]$, the one turn map M, is obtained by composing the corresponding transfer maps $M_1, \ldots, M_m$

$$\mathbf{x}' = M(\mathbf{x}) = M_m \circ M_{m-1} \circ \ldots \circ M_2 \circ M_1(\mathbf{x}), \quad \mathbf{x} \equiv \mathbf{x}(0), \ \mathbf{x}' \equiv \mathbf{x}(s_m) \tag{2}$$

The orbit $\{\mathbf{x}, \mathbf{x}_1, \mathbf{x}_2, \ldots, \mathbf{x}_t, \ldots\}$ on the chosen $s = 0$ section of the lattice is obtained by iterating M. Approximating the transfer map for any magnet of length ℓ with one or two symmetric kicks preserves the symplectic character of the map and the errors are of order ℓ^2 and ℓ^3 respectively. We recall that a map $M(\mathbf{x})$ is symplectic if its jacobian matrix $L_{ij} = \partial M_i / \partial x_j$ is symplectic, namely if it satisfies

$$L J \tilde{L} = J \tag{3}$$

where J is an antisymmetric matrix whose nonvanishing elements are $J_{12} = J_{34} = 1$, $J_{21} = J_{43} = -1$. Low order truncations of the polynomial map M may be computed by composing and truncating subsequently at order N all the transfer maps. Tracking with the truncated map is much faster, but the errors grow by approaching the dynamic aperture A, and crossing a resonance. A scaling law $(||\mathbf{x}||/A)^{N+1}$ is expected for the error after one turn; the most visible effect of the truncation error is the loss of symplecticity. We considered a 2D model of SPS with strong sextupoles (the set up of the machine for diffusion experiments) described by 8 Hénon maps with an overall linear tune $\nu = 26.637$. The truncation from order 10 to 20 gives comparable results; orders higher than 25 cannot be reached because of round off errors and at lower orders the scaling law for the error is confirmed. On the big chain of islands before the dynamic aperture the loss of symplecticity is quite evident after a few thousands of iterations as shown by Figure 1.

Various methods have been proposed to recover a symplectic map from a polynomial truncation: they are based on the direct use of Lie series[4,5] or on normal forms.[6,7] Codes to compute the truncated map and the normal forms have been developed.[8,9] A symplectic map with linear part L has the representation

$$M(\mathbf{x}) = Le^{D_K}\mathbf{x} = e^{D_G}\mathbf{x} \tag{4}$$

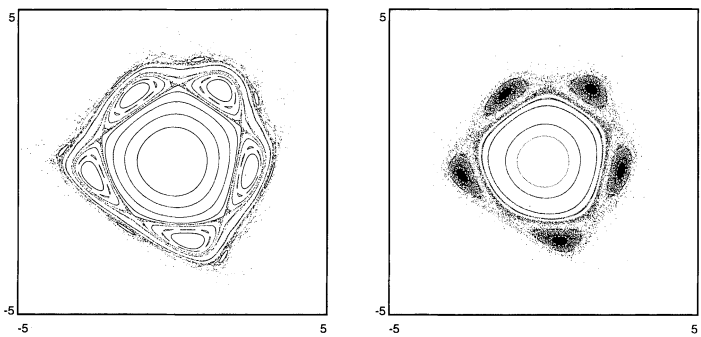

FIGURE 1 Comparison of tracking on 4000 turns between the SPS map (left) and its order 20 truncation (right).

where $K(\mathbf{x})$ is a scalar function and D_K denotes its Lie derivative. Fast recursive algorithms allow to compute K from $L^{-1}M$, and algebraic procedures are used to evaluate G. The map e^{D_G} has trivial iterations and G is its invariant; for a generic map M the series defining K and G are asymptotic[10] (the map $(x, p + x^2)$, for which $K = -x^3/3$, is generic if we compose it with $(x + p^2, p)$). A truncated map of order N determines uniquely the functions K and H up to order $N + 1$ and leaves their higher order terms arbitrary.

3 THE NORMAL FORMS

The basic idea of normal forms is to find a change of coordinates such that the map exhibits an explicit symmetry group $\mathcal{G}$: this is the group generated by the linear part of the map or any of its subgroups. For a 2D map written in the Courant Snyder coordinates $\mathcal{G}$ is just the group of continuous or discrete rotations $R(\omega)$ in the phase plane (x, p_x). For a 4D map $\mathcal{G}$ is the group of the continuous or discrete rotations in the phase planes (x, p_x) and (y, p_y). Assuming that the linear part L of the one turn map M is in block diagonal form $L = L_1 \oplus L_2$, a similarity transformation $T = T_1 \oplus T_2$ brings L to a rotation $R(\omega_1, \omega_2) = R(\omega_1) \oplus R(\omega_2)$, where the standard parametrization of T_k is $(T_k)_{11} = \beta_k^{1/2}$, $(T_k)_{22} = \beta_k^{-1/2}$, $(T_k)_{12} = 0$, $(T_k)_{21} = -\alpha\beta_k^{-1/2}$ for $k = 1, 2$. After the change of coordinates $\mathbf{x} \to T^{-1}\mathbf{x}$ the linear part of the map $M \to TMT^{-1}$ is a rotation; a FODO cell with a thin sextupole is described by the 4D Hénon map. The normal form with respect to the group $\mathcal{G}$ generated by the linear part $R \equiv R(\omega_1, \omega_2)$, is a map U invariant with respect to $\mathcal{G}$

$$U(R\mathbf{x}) = RU(\mathbf{x}) \quad \longrightarrow \quad U(R^n\mathbf{x}) = R^nU(\mathbf{x}). \tag{5}$$

A symplectic map U in normal form is represented by

$$U(\mathbf{x}) = Re^{D_H}\mathbf{x} \tag{6}$$

where $H(\mathbf{x}) = O(|\mathbf{x}|^3)$, called the interpolating hamiltonian, is invariant with respect to U, which has trivial iterations

$$\begin{cases} U^{\circ n} = R(n\omega)e^{nD_H} \\ H(U\mathbf{x}) = H(Re^{D_H}\mathbf{x}) = H(e^{D_H}\mathbf{x}) = H(\mathbf{x}) \end{cases} \tag{7}$$

Letting $\Phi(\mathbf{x})$ be a change of coordinates starting with the identity, the functional equation defining Φ and U is

$$M \circ \Phi(\mathbf{x}) = \Phi \circ \left(Re^{D_H}(\mathbf{x}) + E(\mathbf{x}) \right) \tag{8}$$

where Φ is a polynomial map of order N and H is a polynomial of order $N+1$. The remainder E of order $N+1$ gives the discrepancy between the map M and its normal form U. Both U and H are determined recursively by the map M truncated at order N. The higher order terms of M contribute to the remainder E. The series though divergent as $N \to \infty$ have an asymptotic character.[11,12] Using the action angle coordinates

$$\begin{aligned} x &= \sqrt{2J_1}\cos\theta_1, \quad y = \sqrt{2J_2}\cos\theta_2, \\ p_x &= -\sqrt{2J_1}\sin\theta_1, \quad p_y = -\sqrt{2J_2}\sin\theta_2 \end{aligned} \tag{9}$$

the hamiltonian H reads

$$H = \sum_{k_1,k_2} h_{k_1,k_2}(J_1, J_2)\cos(k_1\theta_1 + k_2\theta_2 + \delta_{k_1,k_2}) \tag{10}$$

where h_{k_1,k_2} has a Taylor expansion in $J_1^{1/2}$ and $J_2^{1/2}$ starting with $J_1^{|k_1|/2} J_2^{|k_2|/2}$. The rotation R leaves J_1, J_2 invariant ad translates the angles $\theta_1 \to \theta_1 + \omega_1$, $\theta_2 \to \theta_2 + \omega_2$. The invariance with respect to the group generated by R implies that only the Fourier components satisfying

$$k_1\omega_1 + k_2\omega_2 = 2\pi\,\ell \tag{11}$$

do contribute in (10). Letting $\omega = (\omega_1, \omega_2, -2\pi)$ and $\mathbf{k} = (k_1, k_2, \ell)$, one interprets (11) as an orthogonality condition $\omega \cdot \mathbf{k} = 0$ and three cases are distinguished: nonresonant $\mathbf{k} = 0$, single resonance $\mathbf{k} = \ell\mathbf{k}_1$, double resonance $\mathbf{k} = \ell_1\mathbf{k}_1 + \ell_2\mathbf{k}_2$ where $\mathbf{k}_1, \mathbf{k}_2$ are integer linearly independent vectors.

3.1 Nonresonant Case

The tunes $\nu_1 = \omega_1/(2\pi)$, $\nu_2 = \omega_2/(2\pi)$ are irrational and have an irrational ratio. The hamiltonian H has only the $k_1 = k_2 = 0$ Fourier component namely $H = h_{00}(J_1, J_2)$ and the invariants are J_1, J_2. The frequencies are given by

$$\Omega_i(J_1, J_2) = \omega_i + \frac{\partial h_{00}}{\partial J_i}(J_1, J_2), \quad i = 1, 2 \tag{12}$$

3.2 Single Uncoupled Resonance

A tune is rational $\nu_1 = p_1/q_1$, the other ν_2 is irrational and $\mathbf{k} = \ell\,(q_1, 0, p_1)$. The hamiltonian H has $k_1 = \ell q_1,\ k_2 = 0$ Fourier components and the leading terms are

$$H = h_0(J_1, J_2) + c J_1^{q_1/2} \cos(q_1\theta_1 + \delta). \tag{13}$$

The invariants are $H,\ J_2$. For a quasiresonant frequency $\omega_1 = 2\pi\ p_1/q_1 + \epsilon_1$ the same resonant normal form may be computed: in this case h_{00} has a linear term $h_0 = \epsilon J_1 + \ldots$.

3.3 Single Coupled Resonance

Both tunes are irrational and their ratio is rational: $\nu_1 = q_1\nu,\ \nu_2 = q_2\nu$ with ν irrational so that $\mathbf{k} = \ell(q_2, -q_1, 0)$. The contributing Fourier components are $k_1 = \ell q_2,\ k_2 = \ell q_1$ and the leading terms are

$$H = h_0(J_1, J_2) + c J_1^{q_1/2} J_2^{q_2/2} \cos(q_2\theta_1 - q_1\theta_2 + \delta). \tag{14}$$

With a canonical change of coordinate $(\theta_1, \theta_2, J_1, J_2) \to (\vartheta_1, \vartheta_2, I_1, I_2)$ where $\vartheta_1 = q_2\theta_1 - q_1\theta_2$ one has $H = H(\vartheta_1, I_1, I_2)$ and $I_2 = q_1 J_1 + q_2 J_2$ is an invariant.

3.4 Double Resonance

The simplest case occurs when both tunes are rational $\nu_1 = p_1/q_1$ and $\nu_2 = p_2/q_2$ where q_1, q_2 have no common divisors. The vectors orthogonal to ω are $\ell_1(q_1, 0, p_1)$ and $\ell_2(0, q_2, p_2)$. The hamiltonian H is no longer integrable and its leading term is

$$H = h_0(J_1, J_2) + c_1 J_1^{q_1/2} \cos(q_1\theta_1 + \delta_1) + c_2 J_2^{q_2/2} \cos(q_2\theta_2 + \delta_2). \tag{15}$$

This hamiltonian has $4q_1q_2$ critical points whose stability has been analyzed.[13,14]

Up to the strongly chaotic regions the orbits of the map are close to the orbits of the interpolating hamiltonian, which belong to invariant manifolds. In the neighborhood of a double resonance the manifold $H = E$ is 3D.

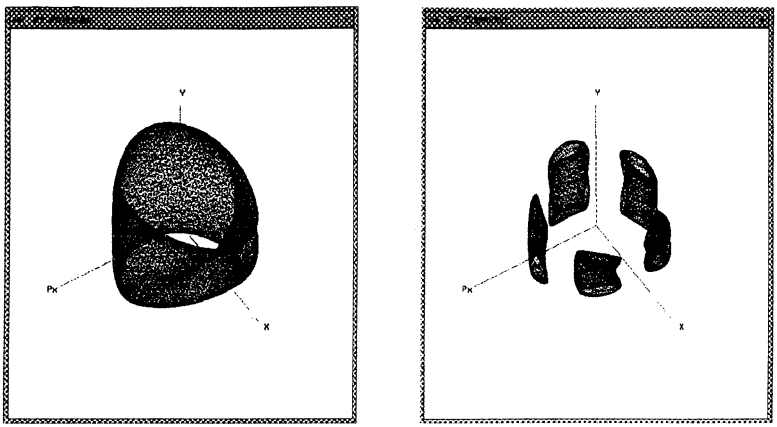

FIGURE 2 Orbits of the 4D Hénon map: (x, p_x, y) projection The left side refers to $\nu_x = (\sqrt{5}-1)/2$, $\nu_y = (\sqrt{3}-1)/2$ and initial point $x = .28$, $y = .2$, $p_x = p_y = 0$ the right side to $\nu_x = .202$, $\nu_y = (\sqrt{5}-1)/2$ and initial points $x = .18$, $y = .0464$, $p_x = .04$, $p_y = 0$.

For a single resonance, the presence of a second invariant J_2 foliates $H = E$ into 2D invariant manifolds. In the non resonant case $H = E$ is foliated by $2D$ tori labeled by the invariants J_1, J_2. Intersecting these manifolds with a moving hyperplane (ordinary 3D space) is a good strategy to visualize them (a surface of 3D space is well described by its intersections with a moving plane). Faster procedures such as the projection on a 3D space have been proposed to analyze the data of tracking.[14,15]

The nature of the orbits emerges by considering H as a perturbation of the hamiltonian $h_{00}(J_1, J_2)$, whose orbits belong to the 2D torus. Topologically the 2D torus is a square in the θ_1, θ_2 plane with identified opposite sides; its embedding in a 3D space is a cylinder with identified basis.

The orbit of the time one map $\theta_1' = \theta_1 + \Omega_1$, $\theta_2' = \theta_2 + \Omega_2$ is dense if Ω_1, Ω_2, defined by (12) are nonresonant. The closure of the orbit is a set of q_1 vertical lines or a single line made of diagonal segments with identified ends or a set of $q_1 q_2$ points if Ω_1, Ω_2 satisfy a single uncoupled, coupled or double resonance condition respectively. The projection of the torus in a 3D space is a cylinder with identified basis and the closure of the orbits is correspondingly the cylinder itself, q_1 vertical lines, a single line winding on the cylinder or $q_1 q_2$ points. Adding the angle dependent term to h_{00} the q_1 lines split into q_1 hyperbolic lines and q_1 elliptic lines, surrounded by

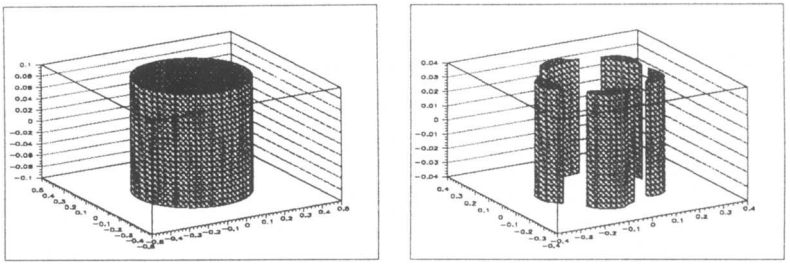

FIGURE 3 Normal forms surfaces for the Hénon map: (x, p_x, y) projection. The parameters are the same as for Figure 2.

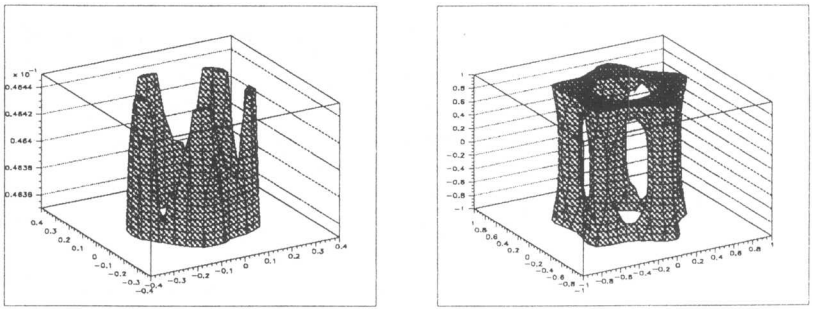

FIGURE 4 Normal forms surface $H = E : (x, p_x, y)$ section. The left side refers to the Hénon map with the same parameters as Figure 2, right side. The right side shows the surface $H = .001$ of the hamiltonian $H = .02\ J_1 - .1\ J_1^2 + .001\ (J_1 J_2 + J_2^2) + .05\ J_1^{5/2} \cos(5\theta_1)$.

cylinders with base $H(\theta_1, J_1, J_2 = 0)$ on planes parallel to the x, p_x plane and $|y| \leq \sqrt{2J_2}$; the $q_1 q_2$ fixed points split into the $4q_1 q_2$ critical points of (15). In Figure 2 we show the projection of the orbits of the Hénon map for non resonant and quasiresonant frequencies; in Figure 3 the projections of the corresponding invariant manifolds given by the normal forms are shown.

The surface obtained by section of the invariant manifold $H = E$ with the hyperplane $p_y = 0$ is shown in Figure 4 (left) for the same Hénon map as Figure 3 (right); a similar picture would be obtained for frequencies close to a double resonance. In the case of a single resonance the $p_y = 0$ sections of

the additional invariant J_2 are the y =const. planes; they intersect the surface $H = E$, $p_y = 0$ on curves surrounding the y axis and on chains of islands.

4 TUNES AND INVARIANT ACTIONS

If the linear frequencies are not doubly resonant the hamiltonian H depends on one angle $H = H(J_1, J_2, \theta_1)$. A locally defined canonical transformation $\theta_1, J_1 \rightarrow \Theta_1, J_1$ and $\Theta_2 = \theta_2, J_2 = J_2$ allows to drop the angle dependence on the hamiltonian $H = \hat{H}(J_1, J_2)$ and to define the nonlinear frequencies Ω_1, Ω_2. The invariant actions J_k and the tunes $\nu_k = \Omega_k/(2\pi)$ are also obtained from a Fourier analysis following a strategy[16] proposed for astronomical models.

4.1 Tunes

The average phase advance APA and the fast Fourier transform FFT determine the tune with a n^{-1} error. A further averaging kills the APA oscillations with n and after extrapolation $n \rightarrow \infty$ the error drops to n^{-2}; combining low order N normal forms with averaged APA one has

$$\delta\nu \sim (x^2 + p_x^2)^{\frac{N+1}{2}}\, n^{-2} \tag{16}$$

for an orbit of length n. The discrete Fourier analysis or interpolation of FFT with a Hanning filter gives a n^{-4} error.[17]

4.2 Invariant Actions

Letting $x = \sqrt{2J}\cos\theta$, $p_x = -\sqrt{2J}\sin\theta$ be the unperturbed action angle variables, the invariant J of a 2D map is obtained by integration on the orbit after reordering the angles as an increasing sequence; the trapezoidal rule gives

$$J = \frac{1}{2\pi}\oint p_x dx = \frac{1}{2\pi}\int_0^{2\pi} J(\theta)d\theta$$

$$= \frac{1}{2\pi}\sum_{k=1}^{n}\frac{j_k + j_{k-1}}{2}(\theta_k - \theta_{k-1}) + O(n\epsilon^3) \tag{17}$$

where $\epsilon = \max|\theta_i - \theta_j| \geq (2\pi)n^{-1}$ and $j_n = j_0, \theta_0 = 0, \theta_n = 2\pi$. The error achieves its minimum n^{-2} for uniformly distributed angles.

The Fourier interpolation of the data $x(t) = \sum_k a_k e^{ik\omega t}$, $p_x(t) = \sum_k b_k e^{ik\omega t}$ from integer to real t gives

$$J = \frac{1}{2\pi}\int_0^T p(t)\dot{x}(t)dt = \mathrm{Im}\sum_{k\geq 1} 2kb_k a_{-k}. \tag{18}$$

The main source of error is due to the truncation of the Fourier series to order $k_{\max}$ and to sampling. For an invariant curve $x(t)$, $p(t)$ are analytic in t and the decrease of the Fourier amplitudes is exponential with $k_{\max}$ on the invariant curves and like $k_{\max}^{-1}$ on a separatrix. Approaching the boundary of a chain of islands the main source of error is the truncation of the Fourier series.

In the quasiresonant case letting $H(J, \theta)$ be the hamiltonian and $E = H(J_0, \theta_0)$ its value for a chosen initial point, the equation of the orbit $J = J(\theta, E)$ is defined implicitly by $H(J, \theta) = E$. Since H is a polynomial in $J^{1/2}$ one has to find its roots and select the real ones. For $E < E_{\mathrm{sep}}$ there are two real roots corresponding to the invariant curve in the inner and outer region with respect to the separatrix; for $E > E_{\mathrm{sep}}$ there are either no real roots or two roots corresponding to the two points where an island is intersected by the half line of polar angle θ. In the first case the invariant is given by

$$J = \frac{1}{2\pi}\int_0^{2\pi} j(\theta, E)d\theta \simeq \frac{1}{n}\sum_{k=0}^{n-1} j(E, \theta_k), \qquad \theta_k = 2\pi\frac{k}{n} \tag{19}$$

The numerical integration error is n^{-2}, since the points are equally spaced; on the separatrix they are chosen to fall on the hyperbolic points, where are the cusps. The accuracy is essentially limited by the asymptotic character of the normal forms: $\delta J \sim n^{-2} + (cJ_0)^{\frac{N+1}{2}}$. A comparison of the methods is shown in Table I for the action of the separatrix of the Hénon map with $\nu = .205$. The accuracy of the Fourier method increases rapidly as we move out from the separatrix and the relative error drops below 10^{-6} for the parameters of Table I, whereas it remains stable for the normal forms unless we get close to the origin. The extension to $4D$ maps is straightforward for the normal forms (J_1 is defined by (19) and J_2 enters $j_1(E, J_2, \theta_1)$ as a parameter) and for the

TABLE I Errors on the invariant $J = .0307$ of the separatrix (area of islands) for the Hénon map with $\nu = .205$, first 4 lines; errors for an outer curve where $J = .0967$, last two lines

n	$k_{\max}$	*error*	n	*error*	n	N	*error*
1000	20	2.3 E-2	100	3.0 E-2	100	5	4.8 E-3
1000	30	1.6 E-2	1000	1.4 E-4	100	7	4.8 E-4
1000	40	1.2 E-2	4000	2.4 E-5	100	8	1.6 E-5
1000	60	1.0 E-2	5000	2.0 E-5	100	10	3.1 E-5
1000	20	2.0 E-5	500	3.1 E-7	50	7	1.2 E-4
1000	30	3.3 E-7	1000	4.2 E-8	50	8	3.6 E-6
	Fourier			Integration		Normal forms	

Fourier method. Indeed letting Γ_1, Γ_2 be the two cycles corresponding to the periods $T_1 = 2\pi/\omega_1$, $T_2 = 2\pi/\omega_2$ the invariants are given by

$$J_k = \frac{1}{2\pi} \oint_{\Gamma_k} (p_x dx + p_y dy) = \frac{1}{2\pi} \int_0^{T_j} (p_x \dot{x} + p_y \dot{y}) dt \tag{20}$$

Fast and accurate computation of the tune, invariants and resonance parameters has several applications: the tune shift minimization allows to correct the multipolar errors and to define a sorting strategy for the random errors.[18]

5 THE DIFFUSION PROBLEM

One of the major sources of instability of the beam is the slow diffusion in action space. The Arnold diffusion has been shown to be negligible in numerical experiments for the Hénon map. Rigorous estimates show that the remainder least value in a disc of radius r is exponentially small with $\dot{r}^{-\alpha}$ where $\alpha < 1/3$; this implies a lower bound[19,20] $T = T_* \exp\left[\left(\frac{r_*}{r}\right)^{\alpha}\right]$ on the stability time. However the analytical estimates of the constants r_*, α are not satisfactory and fits on the tracking data are difficult. Significant diffusion in symplectic maps is observed when the linear frequency is modulated periodically, or stochastically.

Consider a polynomial area preserving map whose linear frequency ω is affected by stochastic fluctuations

$$\begin{pmatrix} x_{n+1} \\ p_{n+1} \end{pmatrix} = R(\omega + \epsilon\xi_n) \begin{pmatrix} x_n + f(x_n, p_n) \\ p_n + g(x_n, p_n) \end{pmatrix} \equiv R(\epsilon\xi_n) \circ F(x_n, p_n) \quad (21)$$

where ξ_n are random variables with zero mean and variance σ. We assume that the deterministic map has no macroscopic resonances up to the dynamic aperture and introduce the nonresonant normal form with the transformation $x = \Phi_x(\Theta, J)$, $p_x = \Phi_p(\Theta, J)$ where Θ, J are the action and angle for the normalized coordinates. Writing the stochastic rotation as a Lie series $R(\epsilon\xi_n)\mathbf{x} = \exp(\epsilon\xi_n D_{\frac{x^2+p^2}{2}})\mathbf{x}$ and performing the change of coordinates one finds that

$$\begin{pmatrix} \Theta_{n+1} \\ J_{n+1} \end{pmatrix} = \exp\big(\epsilon\xi_n D_{V(\Theta,J)}\big) \circ \exp\big(D_{H_0(J)}\big) \begin{pmatrix} \Theta_n \\ J_n \end{pmatrix} \quad (22)$$

where $H_0 = \omega J + h_2 J^2 + \ldots + h_{\frac{N+1}{2}} J^{\frac{N+1}{2}}$. The function $V(\Theta, J)$ is given by

$$V(\Theta, J) = \frac{1}{2}[\Phi_x^2(\Theta, J) + \Phi_p^2(\Theta, J)]. \quad (23)$$

The hamiltonian H which interpolates the map (22) is given by

$$H = H_0(J) + \epsilon\Xi(t)H_1(\Theta, J) + \epsilon^2\Xi^2(t)H_2(\Theta, J) + O(\epsilon^3). \quad (24)$$

The remainder terms of order $J^{1+\frac{N}{2}}$ are assumed to negligible with respect to ϵ^2. The stochastic process $\Xi(t)$ is defined according to $\Xi(t) = \xi_n$ for $t \in [n, n+1]$. The Fourier coefficients $h_{1,k}$ of H_1 are related to the Fourier coefficients v_k of V by the following relation

$$h_{1,k}(J) = v_k(J)\frac{\frac{k\Omega(J)}{2}}{\sin\frac{k\Omega(J)}{2}}. \qquad k \neq 0 \quad (25)$$

The subsequent step consists in writing the Liouville equation for the time evolution of the probability density

$$\frac{\partial \rho}{\partial t} = \omega \frac{\partial \rho}{\partial \Theta} + \epsilon \Xi[\rho, H_1] + \epsilon^2 \Xi^2[\rho, H_2]. \tag{26}$$

The equation simplifies because the autocorrelation $\langle \Xi(t+\tau)\Xi(t)\rangle$ of the process $\Xi(t)$ vanishes for all τ not in the interval $[t]-t \leq \tau < t-[t]+1$, where it is equal to σ^2. The separation of the angle and action diffusion time scales allows to write an equation for the time evolution of the action density. Indeed from $\langle(\Delta\Theta)^2\rangle \propto (d\Omega/dJ)^2 \epsilon^2 n^3$ and $\langle(\Delta J_n)^2\rangle \propto \epsilon^2 n$ follows that the angle relaxation time is $\tau_\Theta \sim \epsilon^{-2/3}$ while the action diffusion time is $\tau_J \sim \epsilon^{-2}$. Angle averaging is justified as soon as the angle has relaxed and it has been shown that if we split the density into an average ρ_0 and a fluctuating part, then for $t \gg \epsilon^{-2/3}$ the average density ρ_0 satisfies a Fokker-Planck equation

$$\frac{\partial \rho_0}{\partial t}(J,t) = \frac{\partial}{\partial J} D(J) \frac{\partial \rho_0}{\partial J}(J,t),$$

$$D = \frac{\epsilon^2 \sigma^2}{2} \frac{1}{2\pi} \int_0^{2\pi} \left(\frac{\partial V}{\partial \Theta}(\Theta, J) \right)^2 d\Theta \tag{27}$$

where an absorbing boundary condition is imposed at the action value J_A corresponding to the dynamic aperture. The agreement between the simulation and the solution of (27) is excellent up to the dynamic aperture when no big islands are present, as shown by Figure 5 left for the Hénon map. The theory extends a 4D map and letting $J = (J_1, J_2)$ the equation for the action density $\rho(J,t)$ reads

$$\frac{\partial \rho_0}{\partial t}(J,t) = \frac{\partial}{\partial J_i} D_{ik}(J) \frac{\partial \rho_0}{\partial J_k}(J,t),$$

$$D_{ik} = \frac{\epsilon^2 \sigma^2}{2} \frac{1}{(2\pi)^2} \int_0^{2\pi} \frac{\partial V}{\partial \Theta_i} \frac{\partial V}{\partial \Theta_k} d\Theta_1 d\Theta_2 \tag{28}$$

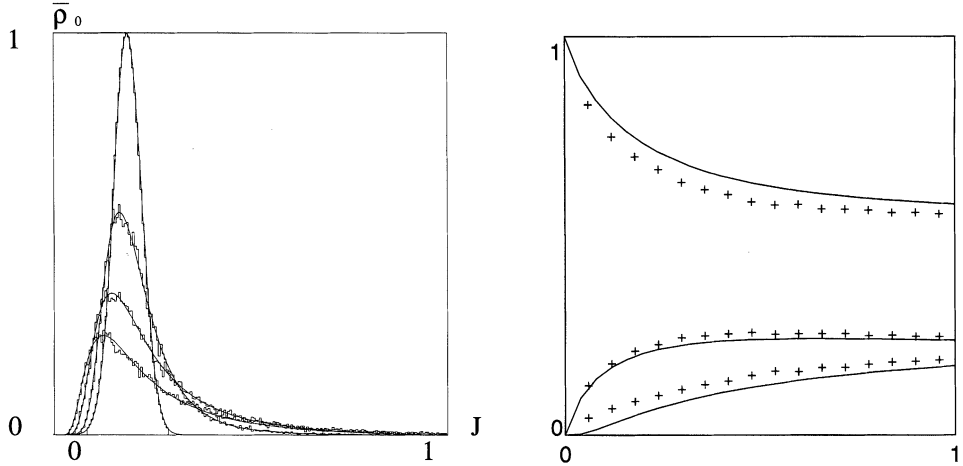

FIGURE 5 Right side: density evolution $\rho(J, n)$ for the Hénon map with $\omega = \pi(\sqrt{5}-1)$, $\epsilon = 2\pi\ 10^{-3}$ against J/J_A for $n = (0, 2, 6, 12)10^3$ (left side). Right side: integrated density time evolution for the hamiltonian $H = -.06\ J(1 + .01\ \xi(t)) + .003\ J^2/2 + .3\ J^2 \cos(4\Theta)$ in the outer (top curve), islands (middle curve) and inner (bottom curve) regions, against $t/t_{\max}$.

The diffusion of action for 2D maps with a chain of islands can be treated by using the quasiresonant normal forms and the transformation $\theta, J \to \Theta, J$ to the invariant action, illustrated in the previous section. We have found that the agreement between the solution of the corresponding F.P. equation and the simulation is still satisfactory[21] as shown by Figure 5 right, where we compare the time variation of the density integrated on inner, outer and the islands region, for the stochastically perturbed interpolating hamiltonian of a map with a forth order resonance. Similar results have been obtained for the diffusion induced by a periodic modulation of the tune[22,23] by using the adiabatic theory.[24]

Acknowledgements

This work was partially supported by EC Human Capital and Mobility contract Nr. ERBCHRXCT940480. Thanks to E. Todesco, A. Bazzani, F. Brini for useful discussions.

References

[1] W. Scandale and G. Turchetti, editors, *Nonlinear problems in future particle accelerators*, Nonlinear problems in future particle accelerators, World Scientific, (1991).
[2] A. Bazzani, E. Todesco, G. Turchetti and G. Servizi, CERN Yellow Report, **94–02** (1994).
[3] A. Bazzani, S. Siboni and G. Turchetti, *Physica D*, **76**, 8 (1994).
[4] A. Dragt and J.M. Finn, *J. Math. Phys.*, **17**, 2215 (1976).
[5] A. Dragt and J.M. Finn, *Nuc. Instrum. Methods Phys. Res.*, **A258**, 339 (1987).
[6] A. Bazzani, G. Turchetti, P. Mazzanti and G. Servizi, *Il Nuovo Cimento*, **B102**, 51 (1988).
[7] E. Forest, M. Berz and J. Irwin, *Part. Accel.*, **24**, 91 (1989).
[8] M. Berz, *Nucl. Instr. and Methods*, **A298**, 437 (1990).
[9] A. Bazzani, M. Giovannozzi and E. Todesco, *Comp. Phys. Comm.*, **86**, 199 (1995).
[10] J. Moser, *Lectures in Hamiltonian Dynamics*, Mem. Am. Math. Soc., **81** (1970).
[11] G. Turchetti, *Methods and Applications of Nonlinear Dynamics*, A Saenz Editor, World Scientific, 91–154, (1988).
[12] A. Bazzani, M. Giovannozzi, G. Servizi, E. Todesco and G. Turchetti, *Physica D*, **64**, 66 (1993).
[13] E. Todesco, *Local analysis of formal existence and stability of fixed points in 4D symplectic mappings*, Physica D, in press (1996).
[14] E. Todesco, Analysis of resonant structures of four-dimensional symplectic mappings, using normal forms, Phys. Rev. E, **50**, R4298 (1994).
[15] F. Schmidt, *PhD thesis* Hera report, **88–02**, unpublished (1988).
[16] J. Laskar, *Physica D*, **67**, 257–281 (1993).
[17] R. Bartolini, A. Bazzani, M. Giovannozzi, W. Scandale and E. Todesco, submitted to Part. Accel.
[18] M. Giovannozzi, R. Grassi, W. Scandale and E. Todesco, *Phys. Rev. E*, **52**, 3093–3101 (1995).
[19] G. Turchetti, in *Number Theory in Physics*, E.J.M. Luck and P. Moussa, Springer Verlag, 223–234 (1990).
[20] A. Bazzani, S. Marmi and G. Turchetti, *Celestial Mechanics*, **47**, 333 (1990).
[21] F.D. Bonino, tesi di Laurea, Università di Torino, in preparation.
[22] F. Brini, PhD thesis, Università di Bologna (1995).
[23] A. Bazzani and F. Brini these proceedings.
[24] A. Neishtadt, *Sov. Journ. Plasma Phys.*, **12**, 568 (1986).